Biosensors and Bioelectronics 56 (2014) 250–257

Contents lists available at ScienceDirect

Biosensors and Bioelectronics

journal homepage: www.elsevier.com/locate/bios

Rapid screening of protein–protein interaction inhibitors using the protease exclusion assay

Saurabh R. Nirantar *[,1], Xiang Li [1], Jia Wei Siau, Farid J. Ghadessy *

*p53Lab (A*STAR), 8A Biomedical Grove, #06-04/05 Neuros, Singapore 138648, Singapore*

ARTICLE INFO

Article history:
Received 7 November 2013
Received in revised form
13 December 2013
Accepted 26 December 2013
Available online 17 January 2014

Keywords:
Biosensor
Protein–protein interaction
P53–Mdm2 interaction
High throughput screening

ABSTRACT

We have previously developed a sensitive and modular homogenous biosensor system using peptides to detect target ligands. By transposing the basic mechanistic principle of the nuclease protection assay into this biosensor framework, we have developed the protease exclusion (PE) assay which can discern antagonists of protein–protein interactions in a rapid, single-step format. We demonstrate the concept with multiple protein–peptide pairs and validate the method by successfully screening a small molecule library for compounds capable of inhibiting the therapeutically relevant p53–Mdm2 interaction. The Protease Exclusion method adds to the compendium of assays available for rapid analyte detection and is particularly suited for drug screening applications.

1. Introduction

It has been shown that more than 80% of proteins do not exhibit activity in the absence of complex formation, indicating the importance of protein–protein interactions in fundamental cellular processes (Berggard et al., 2007; Veselovsky et al., 2002). This observation has led to the relatively new endeavor of seeking antagonists of protein–protein interactions for therapeutic purposes (Arkin and Wells, 2004). Notable successes include numerous small molecule and peptidic antagonists of the p53–Mdm2 interaction (Shangary and Wang, 2009; Zhao and Bernard, 2013), SM-164 (inhibitor of the XIAP-caspase interaction) (Sun et al., 2008) and ABT-737 (blocks the interaction between Bcl-XL and Bak) (Parrondo et al., 2013).

A large number of these protein–protein interactions are mediated by specialized modular protein domains like PDZ, SH2, and SH3, which bind to cognate peptides in their respective interaction partners (Beuming et al., 2005; Pawson et al., 2001; Petsalaki and Russell, 2008). In addition to the widespread usage of specialized peptide binding domains, it is estimated that in more than 50% of globular protein–protein interactions, the dominant contribution from one protein of the interacting pair can be reduced to a single peptide (London et al., 2010). Similarly, Jochim and Arora (2010) have analyzed the PDB structural database and shown that helical peptide segments form a major constituent of a number of protein–protein interactions which could be susceptible to small molecule inhibitors. Large numbers of peptide mimotopes, which can mimic one binding partner of a protein–protein interacting pair, have been discovered, typically using peptide phage display (Huang et al., 2012). Numerous databases and tools have been created to enable facile study of peptide–protein interactions (Shtatland et al., 2007; Vanhee et al., 2010). These facts point to the salience of peptide–protein interactions in the protein–protein interaction network. It would thus be very useful from a therapeutic perspective if novel methods could be developed to enable rapid and facile screening of drugs which can disrupt peptide–protein interactions (Chen et al., 1993). Prevailing methods such as Enzyme-linked immunosorbent assay (ELISA), Surface plasmon resonance (SPR) and Fluorescence polarization (FP) can be adapted to study protein–protein interaction and inhibitor screening. However, none of these methods fulfill all the criteria desirable for drug screening, such as a homogenous set-up for facile high throughput screening, absence of washing and/or immobilization steps, robustness in the presence of a wide variety of autofluorescent small molecule drugs, presence of serum, cell lysates and other complex fluids, and a turn-on instead of a turn-off signal in response to an inhibitor. For example, ELISA and SPR are time and labor intensive, whilst Fluorescence Polarization is a turn-off method which can suffer interference from autofluorescent drugs or small metabolites (Owicki, 2000). Other homogenous methods such as the protein fragment complementation assay (PCA) typically give a turn-off signal in response to interaction inhibitors and require the fusion of split protein domains to the interacting proteins (Hashimoto et al., 2009). Therefore, in order to meet the requirements of high throughput screening and accelerate the detection of antagonists of protein–protein interaction with high sensitivity and minimal process time, designing a homogenous screening system with high specificity

* Corresponding authors.
E-mail addresses: SNirantar@p53Lab.a-star.edu.sg (S.R. Nirantar), faridg@p53Lab.a-star.edu.sg (F.J. Ghadessy).
[1] These authors contributed equally.

0956-5663/$ - see front matter © 2014 Published by Elsevier B.V.
http://dx.doi.org/10.1016/j.bios.2013.12.060

and robustness is necessary. We have therefore developed such a method by extrapolating the principles of the nuclease protection assay into a protein based system. We demonstrate the method using both fluorescence and enzyme-coupled readout formats. We further validate it in a small-molecule (fragment) screen for inhibitors of the p53–Mdm2 interaction, where it demonstrated high sensitivity and specificity compared with other methods.

2. Materials and methods

Chemicals and reagents were purchased from Sigma Aldrich, unless indicated otherwise. The Mdm2 protein used here is derived from N terminal domain (amino acids 18–125) of wild type Mdm2 protein and engineered with 10 × His tag, the protein was expressed in *E. coli* and purified by immobilized affinity chromatography as described earlier (Brown et al., 2011b). The eukaryotic translation initiation factor 4E (eIF4E) was produced as previously reported (Brown et al., 2007). All synthetic peptides used were obtained from Bio-Synthesis, Inc (USA).

2.1. Experimental verification using fluorescence labeled peptide

The PE concept was first validated by using a peptide (P1) labeled with a fluorophore and quencher pair. The peptide sequence is as follows:

E(EDANS)–SG DDDDR-GK (Dabcyl)-TSFAEYWNLLSP-GS.

In this peptide, the fluorophore 5-((2-Aminoethyl)amino)naphthalene-1-sulfonic acid (EDANS) is conjugated as a side chain to glutamic acid followed by amino acids SG as a linker. DDDDR is an enhanced enterokinase cleavage recognition site (Boulware and Daugherty, 2006). The EDANS quencher 4-(dimethylaminoazo)benzene-4-carboxylic acid (Dabcyl) is conjugated to the side chain of lysine followed by a high affinity peptide sequence (TSFAEYWNLLSP) derived by phage display which binds the p53 binding pocket in the Mdm2 N-terminal domain. In a final volume of 25 μl with 4% DMSO buffered by phosphate buffered saline (PBS) at pH 7.3, 1.33 μM fluorescent labeled peptide (E(EDANS)–SG DDDDR GK (Dabcyl) TSFAEYWNLLSP GS), 152 pM enterokinase and 3.2 μM Mdm2 are present. Apart from these constant reagents, triplicates of varying concentrations of Nutlin, wild type p53 peptide (ETFSDLWKLLS) and a mutant p53 peptide with critical residues mutated to alanine (ETASDLAKLAP) were added to the reaction. Enterokinase was added last, after a 5 min delay to ensure that no premature cleavage of peptide occurs. The resulting reaction was read on a Perkin Elmer plate reader in a 384 well black bottom plate (Greiner) with excitation at 335 nm and emission at 490 nm. Readings were taken every 5 min. The signal was calculated as the difference between emission intensity at reading 3 and 5. Every experiment was repeated three times and the average with standard error was reported.

2.2. Plasmid construction and oligonucleotides

Four plasmids were used in this study. HA–enterokinase plasmid was constructed by inverse PCR (Nirantar et al., 2013) of a codon optimized Tem1–BLIP (D49A) cassette (Genscript) placed in the NdeI XhoI sites of pET28a using the oligonucleotides 1 and 2 as described in Supplementary Table 1. Oligo 1 is a Tem1 reverse oligo whose 5′ partially codes for the intended linker sequence. Oligo 2 is a BLIP forward oligo whose 5′ has 15 bases complementary to oligo 1 for infusion cloning purposes, and codes for the rest of the peptide linker sequence. After the inverse PCR, the PCR product was treated with DpnI, purified and treated using the infusion cloning enzyme (Clontech) to enable intra-molecular infusion, followed by transformation in JM109 HIT competent cells (RBS Biosciences). The HA–TEV plasmid was made as above, using oligonucleotides 3 and 4 (Supplementary Table 1), using the HA–enterokinase plasmid as a template.

The Mdm2–enterokinase sensor was constructed in the same way, except that the Tem1–BLIP (D49A) template used has a linker present between Tem1 and BLIP. Oligonucleotide 5 (Supplementary Table 1) is a reverse oligo, while tandem oligonucleotides 6 and 7 are forward oligos complementary to the linker sequence. Tandem oligonucleotides were used due to the length of the peptide linker to be inserted. The eiF4E–enterokinase sensor was made as the Mdm2–enterokinase sensor, using oligonucleotide 5 as a reverse oligo and oligonucleotides 8 and 9 as tandem forward oligos (Supplementary Table 1).

2.3. Sensor protein production

The relevant plasmid was transformed into SHuffle T7 Express Competent *Escherichia coli* cell (New England Biolabs), the transformed cells were grown overnight in LB medium containing 50 μg/ml kanamycin sulfate at 30 °C under shaking conditions. 1% (v/v) of the overnight culture was inoculated into 250 ml LB medium at 30 °C, and protein expression of the fusion proteins was induced with IPTG at OD600 = 0.7–0.8. After 4 h post-induction at room temperature, the cells were harvested by centrifugation. The washed cell pellets were resuspended in 20 ml 50 mM Phosphate buffer (pH 7.4) and disrupted by sonication using a digital sonifier (Life Technologies, Novex). Sonication was performed for 15 cycles at 5 s/cycle, followed by 10 s cooling after each sonication cycle. The lysed cells were centrifuged at 10,000*g* for 30 min, and the suspension was then collected. The filtered supernatant of cell lysate containing sensor protein with a 6 × His tag was loaded onto a 1 ml Ni Sepharose His Trap column (GE Healthcare). The column was pre-equilibrated with Buffer A (50 mM phosphate buffer, 300 mM NaCl, 30 mM imidazole, pH 7.4). After washing with 10 column volume (CV) of Buffer A, the target sensor protein was eluted at 80% Buffer B (phosphate buffer, 300 mM NaCl, 500 mM imidazole, pH 7.4) over 15 CVs. The recovered sensor protein was stored in −80 °C for further usage.

2.4. HA–enterokinase sensor assay

All reactions were performed in 25 μl PBS with 250 μM substrate (Nitrocefin, Merck) and Greiner Bio 384 well transparent bottom plates were used to hold the reactions. The reaction was monitored using absorbance measurements at OD492 on a Perkin Elmer plate reader every 2 min. The sensor response to enterokinase was first investigated by mixing 5 nM relevant sensors (diluted from 1.25 μM stock) with various amount of enterokinase (0.3 nM–1.2 nM) at room temperature; TEV (1.2 nM) was used as the negative control. Subsequently, the sensor response to anti-HA antibody F-7 (Santa Cruz Biotech) was investigated by adding various amount of HA antibody (3 nM to 10 nM) in the presence of 1.2 nM enterokinase; 10 nM whole mouse IgG was used as the control. Sensor response to various concentrations of free HA peptide (0.8 nM to 8 μM) was carried out in the presence of 1.2 nM enterokinase and 10 nM anti-HA antibody, 8 μM p53 peptide was used as the control. The rate of substrate turnover, typically the OD492 value of read number 3 subtracted from that of read number 5 (OD492 readings were taken every 2 min) was denoted as the signal. Every experiment was repeated three times and the average with standard error was reported.

2.5. Mdm2–enterokinase sensor assay

The reaction was carried out in 25 μl PBS with 5 nM sensor, 0.15 nM enterokinase, 40 nM Mdm2 and 250 μM nitrocefin. Nutlin was used as the positive control and a mutant p53 peptide which cannot bind to Mdm2 was used as the negative control. The reaction was monitored using absorbance measurements at OD492 on a

Perkin Elmer plate reader every 2 min. The signal was calculated from reading 5 minus reading 3. This assay was repeated three times and the average gradient value with standard error was reported.

2.6. Mdm2-binding fragment discovery using Mdm2–enterokinase sensor

The Zenobia fragment library containing 352 compounds was used to test the performance of p53–Mdm2 sensor in high throughput screening(Chessari and Woodhead, 2009). The screening was divided into two steps. In the first step, the screening was carried out at the fixed compound concentration of 800 μM. In the second step, a dose-response experiment of different hits found in the first step was conducted. The reaction was carried out in 25 μl PBS with 5 nM sensor, 0.15 nM enterokinase, 40 nM Mdm2, 3% DMSO and the compounds were varied from 800 μM to 9.8 μM. The OD492 value of read number 3 was subtracted from that of read number 5 (OD492 readings were taken every 2 min) which was designated as signal. These gradients were divided by the gradient of negative control to give the fold change (Eq. 1). This data is represented as fold change (*Y* axis) vs. compound concentrations (*X* axis).

$$\text{Fold change} = \frac{\text{Gradient of Hits (Reading 5} - \text{Reading 3)}}{\text{Gradient of control (Reading 5} - \text{Reading 3)}} \quad (1)$$

2.7. Fluorescence polarization

Fluorescence polarization measurements were performed essentially as described in previous study (Brown et al., 2013). Briefly, in a 100 μl reaction buffered by 0.1% PBS–Tween (pH 7.3), 50 nM of fluorescently labeled p53 derived 12-1 peptide (FAM-RFMDYWEGL-NH_2) which can bind to Mdm2 and 200 nM Mdm2 were added, along with the indicated amounts of competing antagonists. Reactions were carried out in duplicate and the average with standard error was reported. The fluorescence polarization values were determined using a Perkin Elmer plate reader at the excitation/emission wavelengths of 485/535 nm.

2.8. Mdm2–p53 immunoprecipitation and qPCR

The immunoprecipitation of p53 via Mdm2 was carried out essentially as described before (Wei et al., 2013). Briefly, full-length Mdm2 and p53 were synthesized separately in in-vitro translation (IVT) mix, followed by capture of the Mdm2 on magnetic beads via an HA tag. Indicated amounts of the relevant drugs were then added for 1 h followed by IVT synthesized p53 for an additional hour. The complex was washed 6 times followed by Western blotting to detect p53. Measurement of p53–Mdm2 interaction by qPCR was carried out as previously described (Wei et al., 2013), with the exception that Mdm2 N-terminal domain (amino acids 1–125) was used as bait.

3. Results

3.1. Method description and proof-of-concept using a fluorescent detector peptide

The method we have developed is analogous to the ubiquitous nuclease protection assay (Papavassiliou, 2009), wherein detection of protein–DNA interaction is coupled to the inability of a nuclease to degrade DNA occluded by bound protein. The protease exclusion (PE) assay (Fig. 1A) replaces the nuclease with a protease, and the DNA component with a reporter moiety comprising a peptide from a peptide–protein interacting pair (peptide A), an adjacent protease

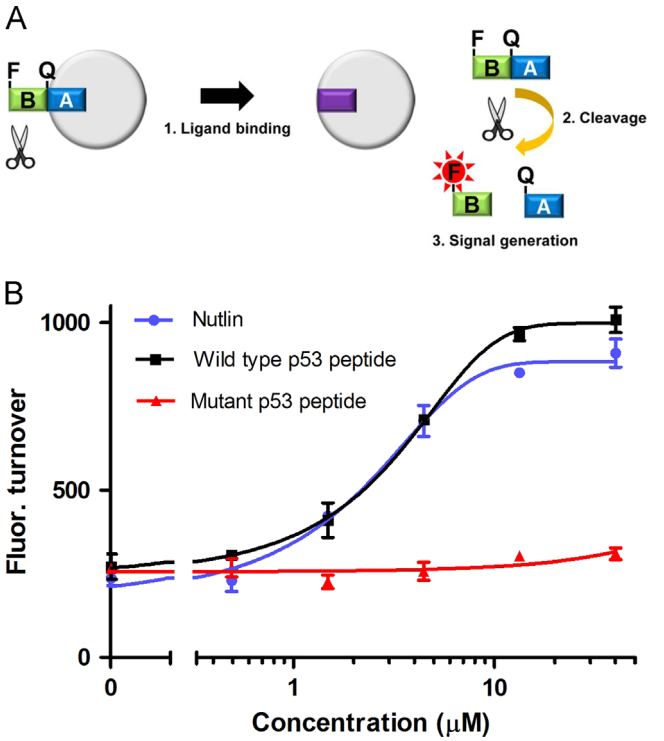

Fig. 1. (A) Schematic representation of the PE assay. The blue segment (region A) of the detector peptide interacts with partner protein (grey circle), the green segment (region B) comprises the protease site. A fluorophore (F) and quencher (Q) are positioned as shown, leading to fluorophore quenching. Close proximity of the two regions prevents protease (scissors) from accessing its cleavage site due to steric hindrance when bound to partner protein (grey circle). When the partner protein is sequestered by a small molecule competitor (purple bar), protease cleavage of detector peptide leads to signal generation. (B) Treatment of protease exclusion fluorescent peptide with Nutlin (light blue), wild type p53 peptide (dark blue), mutant p53 peptide (red) at various concentrations. As expected, Nutlin and the wild type p53 peptide, but not the mutant p53 peptide leads to de-protection of the fluorescent peptide by sequestering Mdm2 N-terminus, leading to cleavage by enterokinase and consequently leading to increased fluorescence development. Thus, fluorescence turnover can be used to monitor Mdm2 inhibition. (For interpretation of the references to color in this figure legend, the reader is referred to the web version of this article.)

cleavage site (peptide B) and a signal generating moiety. Due to the close proximity between A and B, binding of the cognate protein interactant to peptide A prevents protease from binding to its adjacent site B via steric hindrance. Inhibition of peptide A–protein interaction by an antagonist relieves this steric blockage, re-enabling protease access to peptide B, reporter cleavage and signal generation.

We first validated the PE assay using an internally quenched fluorescent detector peptide comprising a p53-derived peptide sequence (TSFAEYWNLLSP) which binds Mdm2 with high affinity (Pazgier et al., 2009) and an adjacent enterokinase cleavage site (DDDDR) (Boulware and Daugherty, 2006). The EDANS–Dabcyl fluorophore–quencher pair was used as the signal generating moiety. The whole peptide sequence is shown below. The p53-derived Mdm2 binding sequence is underlined, while the enterokinase cleavage site is in bold.

N term-E(EDANS)–SG **DDDDR**-GK (Dabcyl)-<u>TSFAEYWNLLSP</u>-GS-C term.

Free Mdm2 is added to the peptide first, resulting in the Mdm2 protein binding to the p53-derived peptide sequence adjacent to the enterokinase site. We hypothesized that binding of the Mdm2 to this region adjacent to the enterokinase site would sterically interfere with enterokinase binding to its recognition site due to the close proximity between the p53 and enterokinase peptide sequences. In the validation experiment, various amounts of p53 peptide, non-

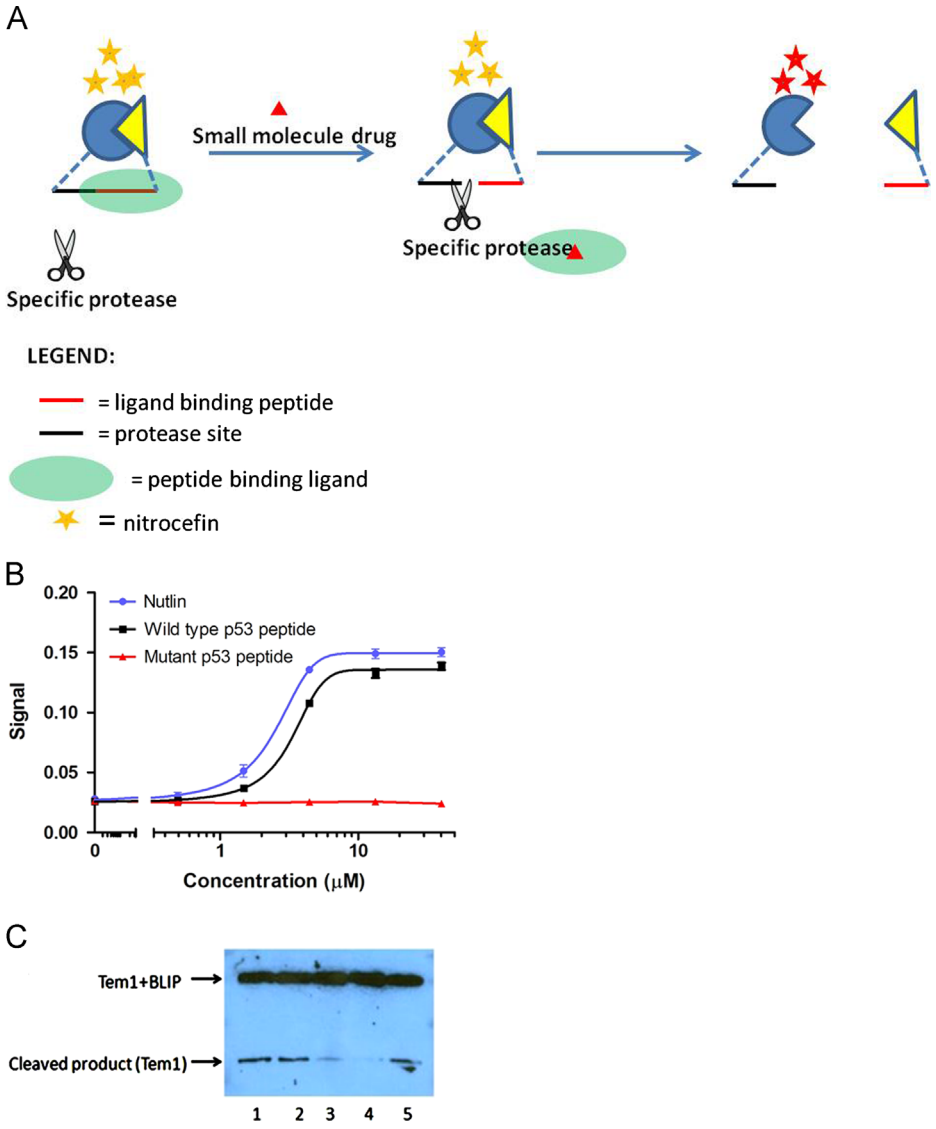

Fig. 2. (A) Schematic representation of the application of "protease exclusion" concept in Tem1–BLIP framework. (B) Substrate turnover rate after treatment of Mdm2–enterokinase sensor with various concentrations of Nutlin, wild type p53 peptide and mutant p53 peptide. (C) Western blot analysis results of different samples in Mdm2–enterokinase sensor assay, lane 1: sensor with enterokinase only, lane 2: sensor with enterokinase, Mdm2 and wild type p53 peptide, lane 3: sensor with enterokinase, Mdm2 and mutant p53 peptide, lane 4: sensor with enterokinase, Mdm2, lane 5: sensor with enterokinase, Mdm2 and Nutlin.

Table 1
The 15 strongest hits obtained from the Mdm2–enterokinase sensor primary screen.

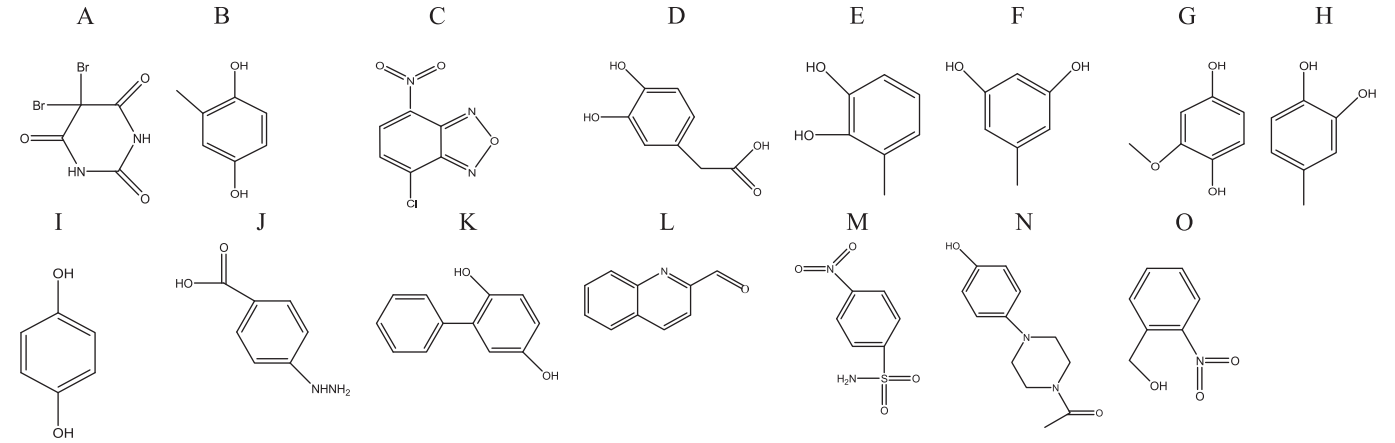

binding mutant p53 peptide as a control or small molecule competitor (Nutlin) (Mouraret et al., 2013; Vassilev et al., 2004), are then added in the presence of Enterokinase. As shown in Fig. 1B, the p53 peptide and Nutlin which are able to reduce the amounts of Mdm2 bound to the reporter peptide promote increased Enterokinase-mediated proteolytic cleavage, resulting in signal generation due to separation of the fluorophore–quencher pair. The degree of cleavage is proportional to the amount of p53 peptide or Nutlin but is insensitive to the presence of non-binding control peptide (Fig. 1B).

3.2. Adaptation into protein biosensor framework

In certain drug screening applications, innate compound fluorescence can potentially interfere with assay readout (Owicki, 2000). To circumvent this issue and broaden the versatility of the PE assay, we incorporated the detector peptide into our previously described modular sensor framework capable of coupling protease activity with enzymatic readout in a one-step homogenous reaction (Nirantar et al., 2013; Banala et al., 2013). Briefly, the detector peptide, placed adjacent to a protease site, forms part of a linker connecting an enzyme (Tem1/β-lactamase) and its inhibitor, BLIP (Fig. 2A). In this configuration, Tem1 is inhibited by BLIP. Cleavage of the peptide linker by protease diminishes BLIP inhibition by reducing effective BLIP concentration. Binding of a protein ligand to its cognate peptide adjacent to the protease site should sterically interfere with protease access to its site. Inhibition of peptide–protein interaction by an antagonist relieves this steric blockage, enabling protease access to peptide linker, reporter cleavage and signal generation (Fig. 2A). A detector peptide (Supplementary Table 2) containing the enterokinase site immediately followed by the Hemagglutinin (HA) epitope tag was introduced into the Tem1–BLIP scaffold. Treatment with enterokinase strongly increases Tem1 enzymatic activity (Supplementary Fig. 1A). Addition of the anti-HA antibody suppresses the response to enterokinase in a dose dependent manner (Supplementary Fig. 1B). The addition of free

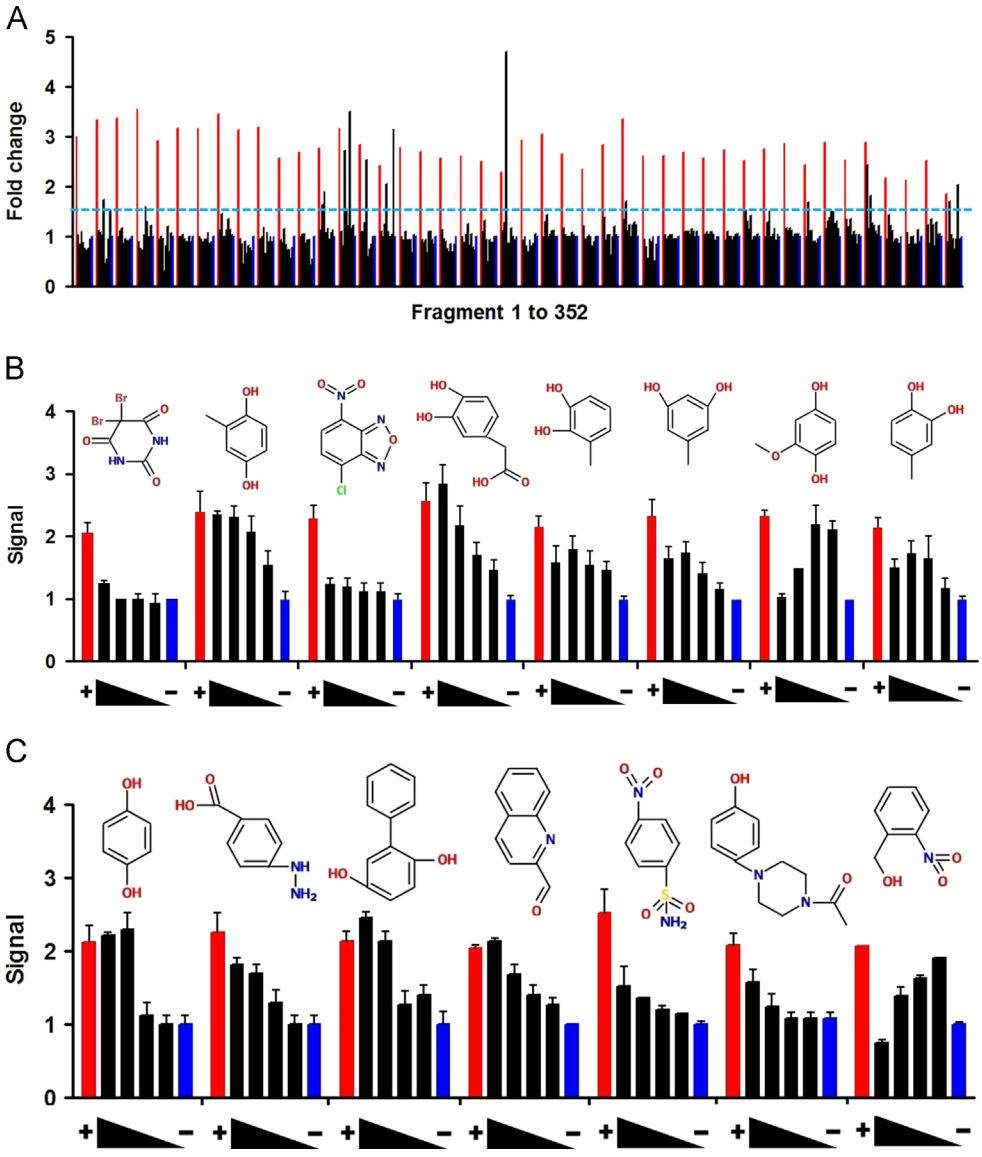

Fig. 3. (A) Primary screening result of all 352 fragments from the Zenobia fragment library. For each plate, drugs from each 8 well column were transposed into a row on the assay plate and each row has a negative (blue) and a positive control (red) flanking the drugs. For each row, the rate of substrate turnover for the negative control was normalized to 1 and the results are as shown. The dotted blue line indicates the cut-off threshold. (B)–(C) Dose response of different hits from primary screening. The rate of substrate turnover obtained by adding decreasing concentrations of various drugs to the Mdm2–enterokinase sensor in the presence of enterokinase is shown. The first bar of each set is a positive control using Nutlin (red, indicated with "+" sign) and the last is a negative control (blue, with "−" sign). The concentrations of the drugs used in the dose response are : 800 μM, 266.7 μM, 88.9 μM and 29.6 μM (black triangles). (For interpretation of the references to color in this figure legend, the reader is referred to the web version of this article.)

HA peptide to a reaction containing both enterokinase and anti-HA antibody resulted in the expected activation, observable by visual inspection (Supplementary Fig. 1C and D). Other combinations such as an HA–TEV protease sensor (Supplementary Fig. 2) have been successfully tested.

3.3. Application to Mdm2 or eIF4E protein–peptide pairs

We next formatted the PE assay for detection of Mdm2 or eIF4E antagonists that inhibit interactions with p53 and eIF4E binding peptides, both relevant targets from a therapeutic perspective (Brown et al., 2011a; Zhou et al., 2012). An Mdm2–enterokinase sensor (see Supplementary Table 2 for sequence) was constructed by inserting a peptide linker with an enterokinase site adjacent to a p53 derived peptide shown to bind Mdm2 (Pazgier et al., 2009). The Mdm2–enterokinase sensor was characterized by adding different amounts of wild type p53 peptide, mutant p53 peptide and Nutlin in the presence of both enterokinase and Mdm2. As shown in Fig. 2B, only the known Mdm2 binders, Nutlin and wild type p53 peptide, and not a control peptide gave rise to signal. Western blot analysis (Fig. 2C) confirmed that signal generation was due to proteolytic cleavage of the scaffolded detector peptide. A similar result was obtained when measuring binding of eIF4e to a relevant detector peptide (sequence in Supplementary Table 2 and Supplementary Fig. 3).

3.4. Drug screening using the Mdm2–p53 protease exclusion sensor

We next evaluated the PE assay for use in drug screening applications by interrogating a small ($n=352$) library of low molecular weight compounds ("fragments") for Mdm2 antagonists (Boyd and de Kloe, 2010; Chessari and Woodhead, 2009). In the primary screen, 15 hits were detected (Table 1 and Fig. 3A), with Nutlin being used as a positive control. Dose-response experiments further confirmed 13 out of 15 fragments as genuine inhibitors in this screen (Fig. 3B and C). The hits were further validated by Fluorescence Polarization as previously described (Brown et al., 2013). Nine of 15 compounds were found to successfully inhibit the p53–Mdm2 interaction to varying degrees (Fig. 4A–C). Of these, fragment G was further validated by an immunoprecipitation assay and found to successfully inhibit full-length Mdm2 interaction with full length p53 (Fig. 5A). There is good agreement between the FP and PE methods. Fragments B, G and I, which were the most potent in the secondary dose-response assay at low concentrations using PE sensors, show similar behavior in the fluorescence polarization assay. However, the protease exclusion sensor was able to detect weaker inhibitors such as fragments J, K, L, M and N which were missed by fluorescence polarization. These fragments were further validated by a sensitive immunoprecipitation based qPCR assay (Wei et al., 2013) and all except fragment N were found to be Mdm2 inhibitors (Fig. 5B), illustrating the greater sensitivity of the method. To rule out the possibility that these compounds cause sensor activation non-specifically, we tested 5 of the strongest hits using the eiF4e PE assay described earlier. None of these resulted in activation (Supplementary Fig. 4), indicating that the Mdm2 protease exclusion sensor had identified specific antagonists of the p53–peptide Mdm2 interaction.

4. Discussion

Peptide–protein interactions are an attractive target for drug development, given their widespread prevalence in the interactome. For example, drugs targeting the p53–Mdm2 interaction are in advanced clinical trials and are promising cancer therapeutics (Zhao and Bernard, 2013). Homogenous one-step techniques enabling high throughput and robust discovery of such drugs are therefore essential. Current techniques such as SPR, ELISA or fluorescence polarization do not meet all desirable criteria because of technical shortcomings. Following from our previous work developing a homogenous protease biosensor, we adapted this concept to enable detection of peptide–protein interactions. The Protease Exclusion concept provides the ability to convert the presence of an inhibitor into fluorescent or enzymatic outputs as shown in this work, thereby increasing the versatility of detection.

Compared with other methods, the protein biosensor framework system has several advantages. For example, the assay can be completed in a shorter duration (between a few minutes to less than an hour depending on the number of wells) than SPR and ELISA, and the biosensor production cost is cheaper than gold chip based methods requiring specialized equipment like SPR. Most importantly, our p53–Mdm2 interaction inhibitor screening results show that the PE biosensor can detect genuine hits (verified by a sensitive pull-down based assay) missed by the fluorescence polarization assay, indicating the high sensitivity and specificity of the PE biosensor. These advantages should enable the PE biosensor to be a useful technique for high throughput drug screening. In addition, detection

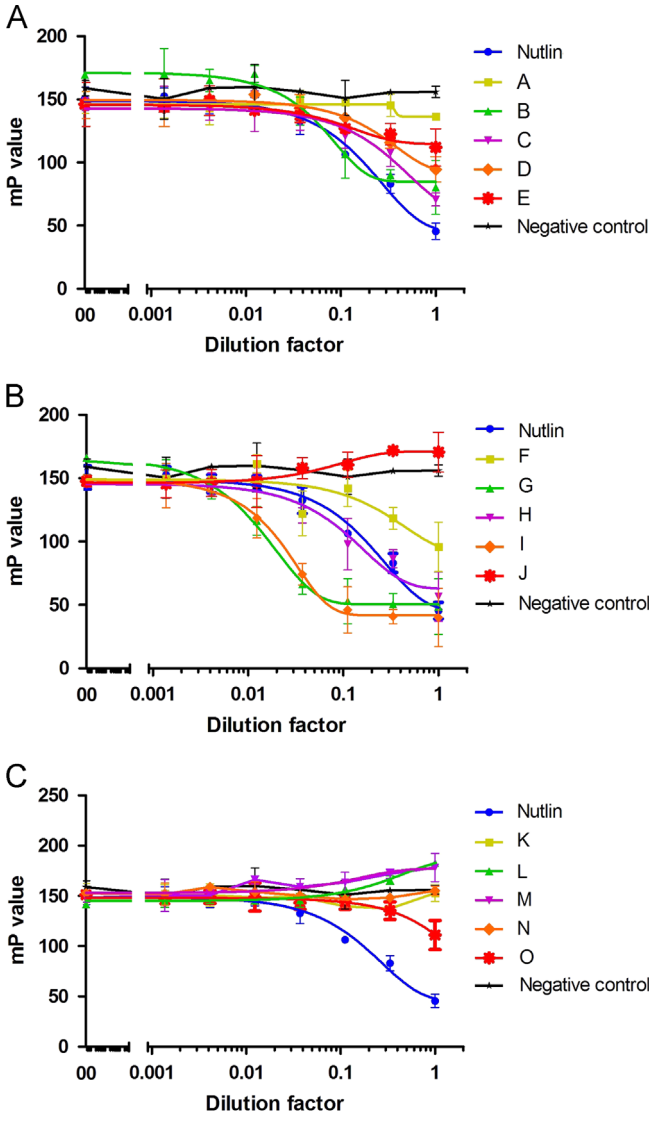

Fig. 4. (A)–(C) 15 positive fragments, a non-reactive fragment (negative control) from the screen and Nutlin (positive control) were tested in a competitive fluorescence polarization assay with a FAM labeled Mdm2 binding peptide (12-1) and purified Mdm2 N terminus, the highest concentration of the drugs is 1 mM while that of Nutlin is 50 μM.

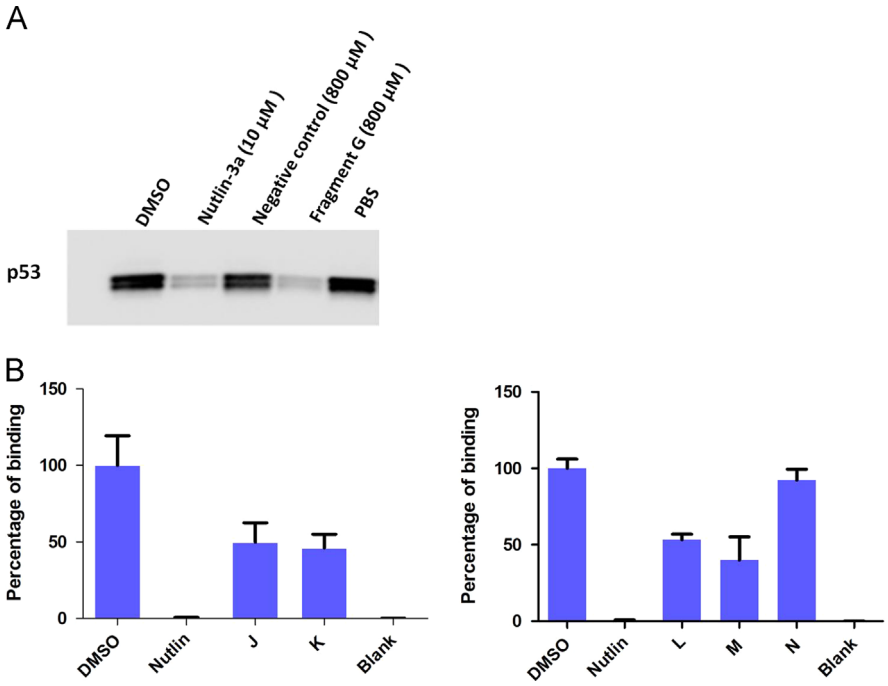

Fig. 5. (A) Mdm2–p53 immunoprecipitation. The fragments that inhibit the interaction will lower the amount of p53 being pulled down as seen above with Nutlin. Fragment G, but not non-reactive fragment(negative control), was able to successfully inhibit the Mdm2–p53 reaction. (B) Determination of p53–Mdm2 interaction and modulation by small molecules using in vitro pull-down and qPCR. Assay measures the amount of DNA (in complex with p53) pulled-down onto beads coated with Mdm2 N-terminal domain protein. Percentage binding denotes the amount of DNA pulled-down in presence of indicated small molecules (10 μM for Nutlin, 1 mM for fragments) compared to DMSO control. Blank reaction indicates DNA pulled-down in absence of Mdm2. Values represent mean ± SD ($n=2$).

and quantification of certain analytes such as the HA epitope tag, (Supplementary Figs. 1 and 2), is feasible using the system. The sensitivity obtained with the HA epitope tag sensor was ~10 nM. While this may not be as sensitive as some other techniques, it is possible to increase the sensitivity of our method by lowering the amount of protease excluding peptide ligand. This will reduce the amount of analyte required to displace the protein, thereby increasing sensitivity, albeit at the cost of lowered maximal *S*/*N* ratio. In applications such as drug screening however, exceptionally high sensitivity may not be required as much as speed, robustness, and convenience which are features of our system.

Given the presence of a protease and a read-out enzyme like β-lactamase in the assay, there is a possibility of aberrant results due to candidate drugs inhibiting these proteins, rather than the intended peptide–protein interaction. However, such drugs will lead to a lowered read-out signal as opposed to an enhanced signal in the case of a genuine peptide–protein inhibitor. Another possible interference comes from drugs whose absorbance profile is similar to that of the chromogenic substrate of β-lactamase, nitrocefin. We encountered some examples of this type of drug in the screening. However, these were easily dealt with by looking at the rate of change of signal rather than absolute values. Thus the biosensor is also robust in the presence of potential confounding factors such as autofluorescent or chromogenic compounds.

Given the very close proximity between the protease cleavage site and the peptide, most proteases should be sterically hindered by most proteins binding their cognate peptides. Thus far, all protein–protease combinations tested, (HA–enterokinase, HA–TEV protease, HA–Thrombin, Mdm2–enterokinase, Mdm2–TEV protease, and eiF4e–enterokinase) using either internally quenched peptides or recombinant Tem1–BLIP scaffolds have resulted in successful protease exclusion.

It is important to note that the enzymatic output need not be limited to β-lactamase. Any enzyme fused to its inhibitor via a suitable peptide linker should serve as a sensor for peptide–protein interaction antagonists. In addition, the possibility of configuring the PE assay for in vivo applications is currently being explored.

5. Conclusions

In summary, we have developed a rapid and versatile methodology that can be used to discern antagonists of protein–protein interactions. The ability to convert the presence of an inhibitor into fluorescent or enzymatic outputs increases the versatility of detection. We anticipate that our method will be effective as a tool in high throughput screening of protein–protein interaction antagonists.

Appendix A. Supplementary material

Supplementary data associated with this article can be found in the online version at http://dx.doi.org/10.1016/j.bios.2013.12.060.

References

Arkin, M.R., Wells, J.A., 2004. Nat. Rev. Drug Discov. 3 (4), 301–317.
Banala, S., Aper, S.J., Schalk, W., Merkx, M., 2013. ACS Chem. Biol. 8 (10), 2127–2132.
Berggard, T., Linse, S., James, P., 2007. Proteomics 7 (16), 2833–2842.
Beuming, T., Skrabanek, L., Niv, M.Y., Mukherjee, P., Weinstein, H., 2005. Bioinformatics 21 (6), 827–828.
Boulware, K.T., Daugherty, P.S., 2006. Proc. Natl. Acad. Sci. USA 103 (20), 7583–7588.
Boyd, S.M., de Kloe, G.E, 2010. Drug Discov. Today: Technol. 7 (3), e173–e180.
Brown, C.J., Cheok, C.F., Verma, C.S., Lane, D.P., 2011a. Trends Pharmacol. Sci. 32 (1), 53–62.
Brown, C.J., Dastidar, S.G., Quah, S.T., Lim, A., Chia, B., Verma, C.S., 2011b. PloS One 6, 8.
Brown, C.J., McNae, I., Fischer, P.M., Walkinshaw, M.D., 2007. J. Mol. Biol. 372 (1), 7–15.
Brown, C.J., Quah, S.T., Jong, J., Goh, A.M., Chiam, P.C., Khoo, K.H., Choong, M.L., Lee, M.A., Yurlova, L., Zolghadr, K., Joseph, T.L., Verma, C.S., Lane, D.P., 2013. ACS Chem. Biol. 8 (3), 506–512.
Chen, J., Marechal, V., Levine, A.J., 1993. Mole. Cell. Biol. 13 (7), 4107–4114.
Chessari, G., Woodhead, A.J., 2009. Drug Discov. Today 14 (13–14), 668–675.

Hashimoto, J., Watanabe, T., Seki, T., Karasawa, S., Izumikawa, M., Iemura, S., Natsume, T., Nomura, N., Goshima, N., Miyawaki, A., Takagi, M., Shin-Ya, K., 2009. J. Biomol. Screen 14 (8), 970–979.
Huang, J., Ru, B.B., Zhu, P., Nie, F.L., Yang, J., Wang, X.Y., Dai, P., Lin, H., Guo, F.B., Rao, N.N., 2012. Nucleic Acids Res. 40 (D1), D271–D277.
London, N., Raveh, B., Movshovitz-Attias, D., Schueler-Furman, O., 2010. Proteins-Struct. Funct. Bioinf. 78 (15), 3140–3149.
Mouraret, N., Marcos, E., Abid, S., Gary-Bobo, G., Saker, M., Houssaini, A., Dubois-Rande, J.L., Boyer, L., Boczkowski, J., Derumeaux, G., Amsellem, V., Adnot, S., 2013. Circulation 127 (16), 1664.
Nirantar, S.R., Yeo, K.S., Chee, S., Lane, D.P., Ghadessy, F.J., 2013. Biosens. Bioelectron. 47 (0), 421–428.
Owicki, J.C., 2000. J. Biomol. Screen 5 (5), 297–306.
Papavassiliou, A.G., 2009. Determination of a transcription factor-binding site by nuclease protection footprinting onto southwestern blots. In: Moss, T., LeBlanc, B. (Eds.), DNA–Protein Interactions: Principles and Protocols, third edition, pp. 201–218.
Parrondo, R., de Las Pozas, A., Reiner, T., Perez-Stable, C., 2013. PeerJ 1, e144.
Pawson, T., Gish, G.D., Nash, P., 2001. Trends Cell Biol. 11 (12), 504–511.
Pazgier, M., Liu, M., Zou, G., Yuan, W., Li, C., Li, J., Monbo, J., Zella, D., Tarasov, S.G., Lu, W., 2009. Proc. Natl. Acad. Sci. USA 106 (12), 4665–4670.
Petsalaki, E., Russell, R.B., 2008. Curr. Opin. Biotechnol. 19 (4), 344–350.
Shangary, S., Wang, S., 2009. Ann. Rev. Pharmacol. Toxicol. 49, 223–241.
Shtatland, T., Guettler, D., Kossodo, M., Pivovarov, M., Weissleder, R., 2007. BMC Bioinf. 8, 280.
Sun, H., Nikolovska-Coleska, Z., Yang, C.Y., Qian, D., Lu, J., Qiu, S., Bai, L., Peng, Y., Cai, Q., Wang, S., 2008. Acc. Chem. Res. 41 (10), 1264–1277.
Vanhee, P., Reumers, J., Stricher, F., Baeten, L., Serrano, L., Schymkowitz, J., Rousseau, F., 2010. Nucleic Acids Res.38(Database issue), D545–551.
Vassilev, L.T., Vu, B.T., Graves, B., Carvajal, D., Podlaski, F., Filipovic, Z., Kong, N., Kammlott, U., Lukacs, C., Klein, C., Fotouhi, N., Liu, E.A., 2004. Science 303 (5659), 844–848.
Veselovsky, A.V., Ivanov, Y.D., Ivanov, A.S., Archakov, A.I., Lewi, P., Janssen, P., 2002. J. Mol. Recognit.: JMR 15 (6), 405–422.
Wei, S.J., Joseph, T., Sim, A.Y., Yurlova, L., Zolghadr, K., Lane, D., Verma, C., Ghadessy, F., 2013. PLoS One 8 (4), e62564.
Zhao, Y., Bernard, D.S.W., 2013. BioDiscovery 8 (4), 1–15.
Zhou, W.Z., Quah, S.T., Verma, C.S., Liu, Y., Lane, D.P., Brown, C.J., 2012. PloS One 7 (10).